PHYLLOTACTIC MODEL LINKING NANO AND MACRO WORLD

HORÁČEK Miroslav[1,*], MELUZÍN Petr[1], KRÁTKÝ Stanislav[1],
URBÁNEK Michal[1,2], BOK Jan[1,3], KOLAŘÍK Vladimír[1]

[1] *Institute of Scientific Instruments of the CAS, Brno, Czech Republic, EU*
[2] *actually with Tomas Bata University in Zlín, Centre of Polymer Systems, Zlín, Czech Republic, EU*
[3] *actually with Tescan, Brno, Czech Republic, EU*
[*] *petr.meluzin@isibrno.cz*

Abstract

Recently, the arrangement of diffraction primitives according to a phyllotactic model was presented. This arrangement was used to benchmarking purposes of the e-beam writer nano patterning. The phyllotactic arrangement has several interesting properties. One of them is related with the coherence between the nano- or microscopic domain of individual optical primitives and the properties of visually perceived images crated by these structures in the macro domain. This paper presents theoretical analysis of the phyllotactic arrangement in the referred context. Different approaches enabling the creation of diffractive optically variable images are proposed. The practical part of the presented work deals with the nano patterning of such structures using two different types of the e-beam pattern generators. One of them is a system with a variable shaped beam of electrons, while the other one is a system with a Gaussian-shaped beam. E-beam writing strategies and the use of inherent spiral patterns for exposure ordering and partitioning are also discussed.

Keywords: Nano patterning, spiral grating structure, phyllotactic pattern, e-beam writer

1. INTRODUCTION

This contribution is related to the planar optical device based on the optical elements arrangement according to a phyllotactic model. This model originally describes positions of seeds in sunflower head [1]. Seed positions in polar coordinates may be defined accordingly to [1] by equation (1), where k is the number of seeds, c is the scale factor and θ_0 is the angular factor (coined the divergence angle in botany). This model was used in various domains in the past decades. Recently, it was used also as a benchmarking pattern for e-beam lithography [2].

$$\{r_k; \vartheta_k\} = \{c \cdot k^{1/2}; k \cdot \vartheta_0\} \tag{1}$$

We present an analysis of the mentioned arrangement from the optical point of view. Characteristic triangles that may be observed in the arrangement are described. Relation between seed distances and periodicity of derived spirals are described. The practical part of the presented work deals with the nano patterning of such structures using e-beam pattern generators.

2. METHOD

One important feature of the phyllotactic arrangement of seeds according to equation (1) is a constant size of the area attributed to each individual seed. The size of this area, let us say the elementary surfaces A_0, can be derived in four different ways. The first way is based on the circular surface around each seed and depends on the scale parameter c, see equation (2). Let us note that three circles around three adjacent seeds are partially overlapping and thus there remains some area in between them that is not covered by any circle.

$$A_0 = \pi \cdot c^2 \tag{2}$$

The second method is derived from the area of elementary annulus that can be imagined as an orbit which can be populated by just one seed, see equation (3). Here, the radii r_{k-1}, r_k, r_{k+1} represent distances of three successive seeds from the pole of the model.

$$A_0 = 2\pi \cdot r_k \cdot \frac{r_{k+1} - r_{k-1}}{2} \tag{3}$$

The third method is derived from the area of the circular sector comprising a single seed, see equation (4). When considering the model with k seeds, the angular distance between two angularly adjacent seeds is $\Delta\theta_k = 2\pi / k$.

$$A_0 = \frac{1}{2} r_k \Delta \vartheta_k \tag{4}$$

Finally, the fourth method defines the size of the elementary surfaces as twice the area of the triangle - edge D_x and altitude L_x in equation (5) - formed by the considered seed and its two closest neighbors. More generally, the size of the elementary area can be derived from triangles which have one vertex in the centre of the considered seed and two vertices in the centre of two seeds along dome derived spirals.

$$A_0 = D_x \cdot L_x \tag{5}$$

These equations and their combination can significantly facilitate the preparation of the seed model and the design and analysis of the discussed seed arrangement.

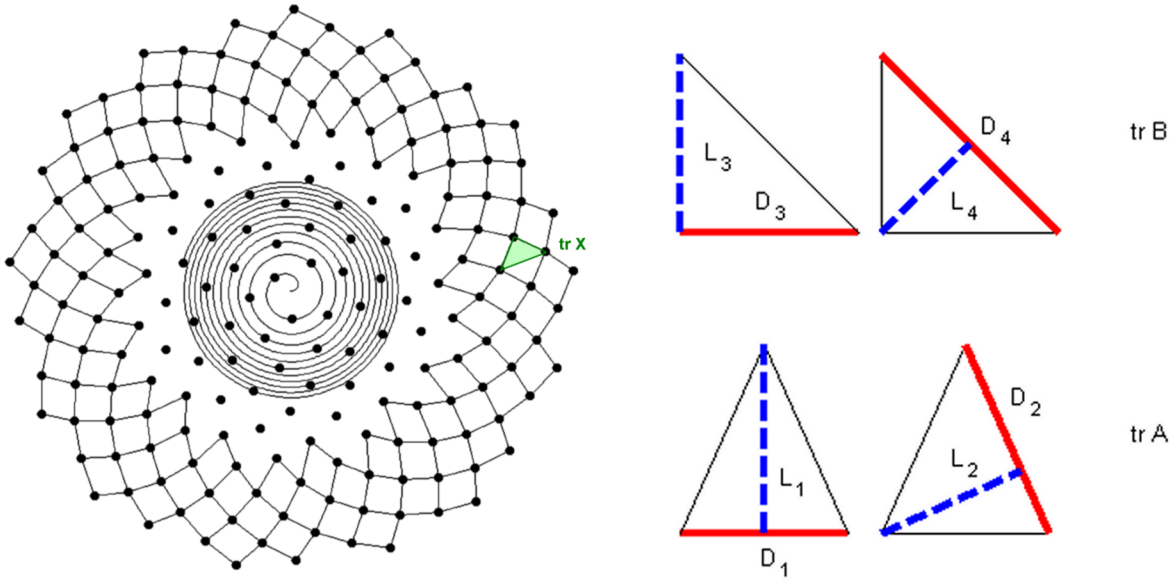

(a) (b)

Figure 1 Vogel's model [1]: a simple arrangement of 400 seeds with highlighted part of the basic spiral, two sets of derived spiral parts and one selected triangle tr X (a); edges and altitudes of two limiting isosceles triangles tr A and tr B (b); see text for details

Figure 1(a) shows a simple seed arrangement of a counterclockwise Vogel's model [1] with 400 seeds. A part of the basic spiral is highlighted, starting from the model pole. Furthermore, two sets of derived spirals (21 spirals of each 21st seed and 34 spirals of each 34th seed) are also featured. Three adjacent seeds form an elementary triangle of the arrangement (tr X). When travelling from the model pole to its circumference,

triangles cyclically change the shape from the first limiting triangle to the second limiting triangle and back to the first one. These limiting triangles are shown in **Figure 1(b)** and described below.

2.1. First limiting triangle - tr A

Figure 1b shows two limiting triangles of the arrangement. The first one (tr A) is an isosceles triangle. Its edges (D_1, D_2) are marked by red color and related altitudes (L_1, L_2) are marked by blue color. The arrangement of seeds of the simple phyllotactic model according to the equation (1) is characterized in that for the most of the seeds there exist two closest neighboring seeds, wherein the positions of these three seeds form the vertices of the common triangle. The shape of these triangles varies with the direction from the pole of the model towards its border; simultaneously, the orientation of the triangles is continuously changing as they are aligned to directions of the derived spirals. The altitudes of the mentioned triangle represents the periodicity of the network of seeds in the vicinity of the given triangle. This periodicity is significant for the construction of the diffraction optical device, since it affects the degree of the light bending on the periodic structure (according to the grating equation).The special lengths and altitudes of the triangle edges are marked as follows: D_1 (base of tr A), L_1 (associated altitude) and D_2 (shoulders of tr A), L_2 (associated altitude). The edge lengths relative to the scale of the phyllotactic model c are expressed by equations (6) and (7) exploiting the introduced constant fm ($fm = \sqrt{5}/2$). The numerical values of the distances are as follows: $D_1 \sim 1.6763c$ and $D_2 \sim 2.0530c$. The values of associated altitudes are derived from the distances using equation (5), their numerical values are $L_1 \sim 1.8741c$ and $L_2 \sim 1.5303c$. The distance D_1 represents the shortest distance between adjacent seeds in the given arrangements while L_1 is its longest periodicity value.

$$\{D_1 ; L_1\} = \left\{c \cdot \sqrt{\pi / fm} ; c \cdot \sqrt{\pi \cdot fm}\right\} \tag{6}$$

$$\{D_2 ; L_2\} = \left\{c \cdot \sqrt{3\pi/(2\,fm)} ; c \cdot \sqrt{2\pi \cdot fm/3}\right\} \tag{7}$$

2.2. Second limiting triangle - tr B

The other limiting triangle (tr B) is an isosceles right-angled triangle, see **Figure 1b**. The special lengths of the triangle edges are marked as follows: D_3 (ordinates of tr B) and D_4 (hypotenuse of tr B); the associated altitudes are L_3 and L_4. Accordingly to equations (8) and (9), their numerical values are: $D_3 \sim 1.7725c$; $D_4 \sim 2.5066c$; $L_3 \sim 1.7725c$; $L_4 \sim 1.2533c$.

$$\{D_3 ; L_3\} = \left\{c \cdot \sqrt{\pi} ; c \cdot \sqrt{\pi}\right\} \tag{8}$$

$$\{D_4 ; L_4\} = \left\{c \cdot \sqrt{2\pi} ; c \cdot \sqrt{\pi/2}\right\} \tag{9}$$

2.3. General triangle - tr C

Generally, the shape of all triangles (tr C) in the arrangement is in between the limiting triangles. The lengths of their edges, denoted $D_{tr\,C,1}$ (the shortest edge), $D_{tr\,C,2}$, and $D_{tr\,C,3}$ (the longest edge), are given by inequalities (10), (11), and (12), respectively. We may conclude that the distance between two adjacent seeds is within the interval (D_1; D_4), that is approximately (1.6763c; 2.5066c).

$$D_1 < D_{tr\,C,1} < D_3 \tag{10}$$

$$D_2 < D_{tr\,C,2} < D_3 \tag{11}$$

$$D_2 < D_{tr\,C,3} < D_4 \tag{12}$$

2.4. Equivalent equilateral triangle - tr 6

It seems interesting to compare the variability of the phyllotactic arrangement with the rigid grid of equilateral triangles (tr 6). The edge D_6 and the altitude L_6 of the equilateral triangle are given by equation (13). These values are related to the scale factor c of the phyllotactic model. The arrangement of this type has the same number of seeds per unit area as the phyllotactic arrangement with the same scale factor c.

$$\{D_6 ; L_6\} = \left\{c \cdot \sqrt{2\pi/\sqrt{3}} ; c \cdot \sqrt{(\pi/2) \cdot \sqrt{3}}\right\} \tag{13}$$

3. EXPERIMENT

The presented method was used for the implementation of algorithms that enable to predict the shape of a diffractive pattern observable when a large size arrangement is prepared as a planar relief microstructure. Two approaches were adopted; the first one is simply based on the simulation of the first order diffraction behavior, see **Figure 2a**; the second one handles also higher diffraction orders and their combinations, see **Figure 3a**. In order to validate the presented method and simulation algorithms we prepared several samples of planar relief structures that exhibit diffractive behavior; one of results is depicted in **Figure 3b**. These structures were prepared using e-beam lithography patterning and standard lithographical process.

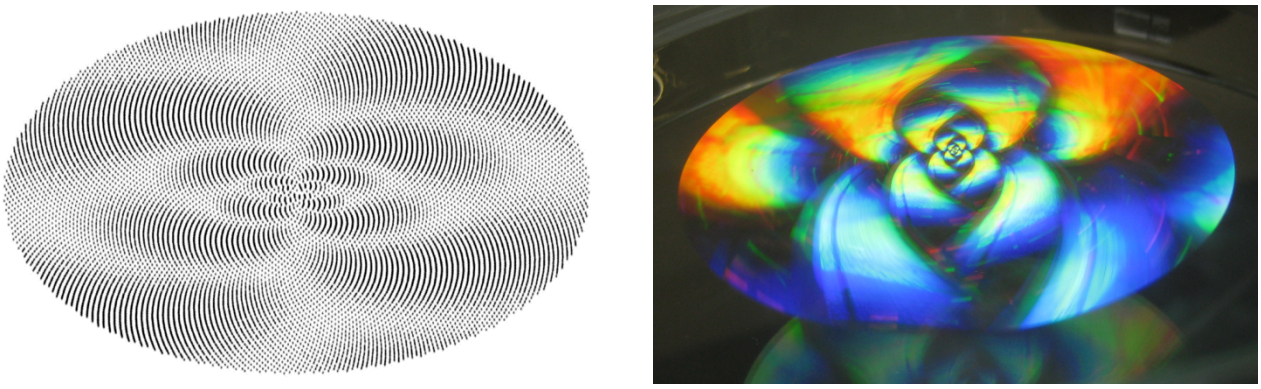

(a) (b)

Figure 2 Diffractive pattern of the phyllotactic arrangement: simulation results (a); real sample photo according to [2] (b)

4. RESULTS AND DISCUSSIONS

Figure 2 shows the comparison of first-order diffraction simulation results and the previously published picture of a real sample [2]. It may be seen that both diffraction patterns present some similarities although the matching is not perfect. This is due to the optically variability of the diffractive pattern that depends on lighting and observation conditions.

Figure 3 shows the comparison of the second simulation algorithm (including higher diffraction orders and their combinations) together with a picture of a real sample. This planar relief structure sample is relatively coarse, with the scale factor $c = 2$ μm. This value ensures the visibility of at least 4 diffraction orders in standard observing conditions. **Figure 3a** showing the simulation results uses different grey values for highlighting locations with particular periodicity. Azimuth orientation of characteristic triangles must lie within predefined limits (in this particular case the tolerance is ±2 degrees) in order to the region is highlighted. In this case the matching between the simulation and the observation is quite close.

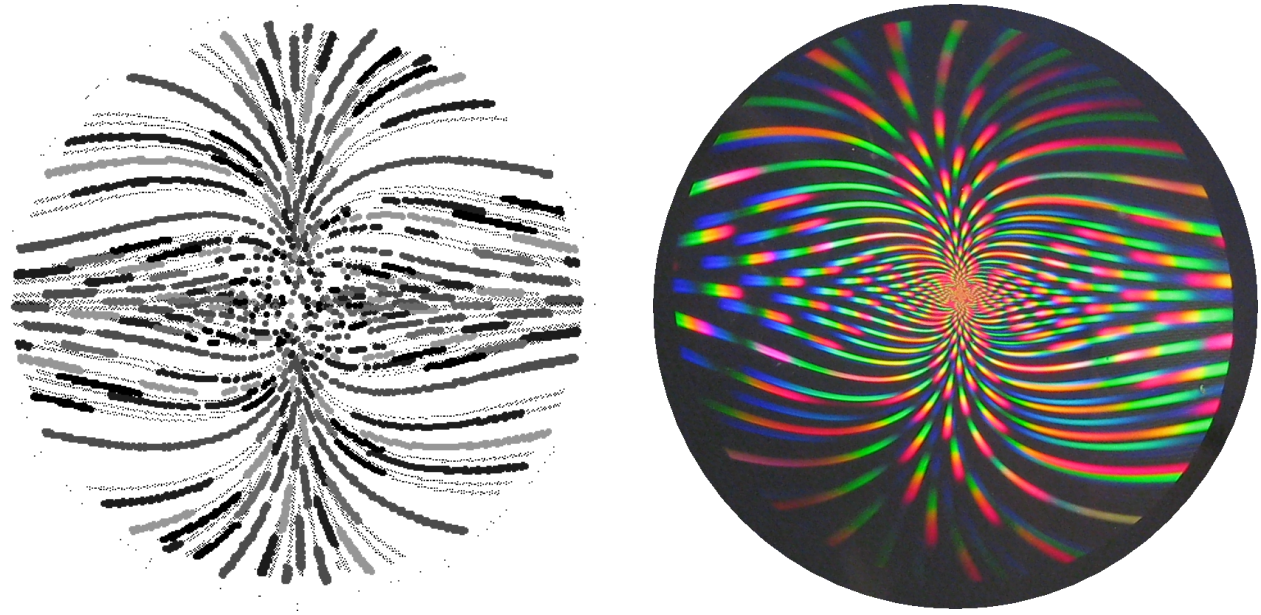

(a) (b)

Figure 3 The diffractive pattern of the planar optical phyllotactic arrangement showing higher-order light diffraction, c = 2 µm, circle diameter 20 mm: model (a); picture of the real sample (b)

5. CONCLUSIONS

We presented the method for analysis and design of large scale phyllotactic arrangements. The method was validated by a planar relief structure that has the expected diffractive functionality. Ongoing and future work covers several related topics, e.g. detailed analysis of the seed model (the shape and the size of particular optical elements), multi-level arrangements (the nesting of two or more phyllotactic models with distinctively different levels of finesse), diffractive optically variable image device [3], elaborated analysis of the diffractive pattern shape and properties, advanced e-beam patterning issues (dosing, partitioning, fractioning, etc.), analysis of structures with the sub lambda / 2 [4] and sub 100 nm value of the scale factor.

ACKNOWLEDGEMENT

The research was partially supported by the TACR project TE 01020233, by MEYS CR (LO1212), its infrastructure by MEYS CR and EC (CZ.1.05/2.1.00/01.0017) and by CAS (RVO:68081731).

REFERENCES

[1] VOGEL, H., A better way to construct the sunflower head. *Mathematical Biosciences* 44 (1979), pp. 179-189.

[2] MELUZÍN, P. *et al.*, Some Other Gratings: Benchmarks for Large-Area E-Beam Nanopatterning. In *NANOCON 2014: 6th Int'l Conference Proceedings*. Ostrava: TANGER, 2014, pp. 246-251.

[3] RENESSE, R. L. van, *Optical Document Security*, *3rd edition*, Boston/London: Artech House (2005), 386 pages, ISBN 1-58053-258-6.

[4] KOLAŘÍK, V. *et al.*, Structural Color of Metallic Surfaces. In *METAL 2014: 23rd International Conference on Metallurgy and Materials*. Ostrava: TANGER, 2014, pp. 962-967.